

Article

PmMYB4, a Transcriptional Activator from *Pinus massoniana*, Regulates Secondary Cell Wall Formation and Lignin Biosynthesis

Sheng Yao, Peizhen Chen , Ye Yu, Mengyang Zhang, Dengbao Wang, Jiahe Liu, Qingqing Hao and Kongsu Ji * 

Co-Innovation Center for Sustainable Forestry in Southern China, Key Laboratory of Forestry Genetics & Biotechnology of Ministry of Education, Nanjing Forestry University, Nanjing 210037, China; yaosheng0817@163.com (S.Y.); pei_jane@126.com (P.C.); yuye1023@163.com (Y.Y.); zhangzhang6660715@163.com (M.Z.); dbw@njfu.edu.cn (D.W.); xiaoheclj@njfu.edu.cn (J.L.); hjh19960812@126.com (Q.H.)

* Correspondence: ksji@njfu.edu.cn

Abstract: Wood formation originates in the biosynthesis of lignin and further leads to secondary cell wall (SCW) biosynthesis in woody plants. Masson pine (*Pinus massoniana* Lamb) is an economically important industrial timber tree, and its wood yield affects the stable development of the paper industry. However, the regulatory mechanisms of SCW formation in Masson pine are still unclear. In this study, we characterized *PmMYB4*, which is a *Pinus massoniana* MYB gene involved in SCW biosynthesis. The open reading frame (ORF) of *PmMYB4* was 1473 bp, which encoded a 490 aa protein and contained two distinctive R2 and R3 MYB domains. It was shown to be a transcription factor, with the highest expression in semi-lignified stems. We overexpressed *PmMYB4* in tobacco. The results indicated that *PmMYB4* overexpression increased lignin deposition, SCW thickness, and the expression of genes involved in SCW formation. Further analysis indicated that *PmMYB4* bound to AC-box motifs and might directly activate the promoters of genes (*PmPAL* and *PmCCoAOMT*) involved in SCW biosynthesis. In addition, *PmMYB4*-OE(over expression) transgenic lines had higher lignin and cellulose contents and gene expression than control plants, indicating that *PmMYB4* regulates SCW mainly by targeting lignin biosynthetic genes. In summary, this study illustrated the MYB-induced SCW mechanism in Masson pine and will facilitate enhanced lignin and cellulose synthesis in genetically engineered trees.

Keywords: *Pinus massoniana*; SCW; *PmMYB4*; AC-Box; lignin biosynthetic



Citation: Yao, S.; Chen, P.; Yu, Y.; Zhang, M.; Wang, D.; Liu, J.; Hao, Q.; Ji, K. *PmMYB4*, a Transcriptional Activator from *Pinus massoniana*, Regulates Secondary Cell Wall Formation and Lignin Biosynthesis. *Forests* **2021**, *12*, 1618. <https://doi.org/10.3390/f12121618>

Academic Editors: Giovanni Emiliani and Alessio Giovannelli

Received: 5 October 2021

Accepted: 22 November 2021

Published: 23 November 2021

Publisher's Note: MDPI stays neutral with regard to jurisdictional claims in published maps and institutional affiliations.



Copyright: © 2021 by the authors. Licensee MDPI, Basel, Switzerland. This article is an open access article distributed under the terms and conditions of the Creative Commons Attribution (CC BY) license (<https://creativecommons.org/licenses/by/4.0/>).

1. Introduction

The formation of wood involves the development of mother cells of secondary xylem differentiated from the vascular cambium, elongation of cells, deposition of the SCW, and programmed cell death (PCD) [1]. Cell walls are the main component of wood, accounting for more than 90% of the dry weight of plants [2]. In plant cells, the cell wall consists mainly of the SCW [3]. During the formation of the SCW, the composition of the cell wall changes significantly, mainly because of the directional arrangement of cellulose, deposition of lignin, and changes in the composition of hemicellulose and proteins [4]. Similarly, the SCW thickness, chemical composition, and structure and the proportions of different cell types determine wood properties [3]. Lignin, cellulose, and hemicellulose are the main components of the SCW. The biosynthesis of these components is not only precisely regulated by structural genes but also strictly regulated by many transcription factors (TFs). Other studies of xylem cell wall biosynthesis in other plants have led to a regulation model that consists of four gene levels: (1) first-layer master switches (NAC genes; NAM, ATAF1/2, and CUC2 genes), (2) second-layer master switches (MYB (myeloblastosis) genes; v-myb avian myeloblastosis viral oncogene homologs), and (3) downstream regulators (TF genes) regulating (4) genes for SCWs [5–10].

Within this network, R2R3-MYB TFs are second-level switch genes that regulate the ectopic deposition of SCW [7]. *MYB46* and *MYB83* are key genes in this group in *Arabidopsis* [11,12], and previous studies have shown that they can promote thickening of the SCW in vessels and fibers [13]. Transcriptional activation analyses and electrophoretic mobility shift assays (EMSAs) have shown that *AtMYB46* and *AtMYB83* bind to the SCW MYB-responsive element (SMRE), which is a 7-bp sequence, to activate downstream TFs and structural genes involved in SCW biosynthesis [14]. Homologous genes of *MYB46* and *MYB83* in other species, such as *EgMYB2* [15], *BplMYB46* [16], *PtMYB4/8* [17], *PtrMYB2/3/20/21* [18], *ZmMYB46*, and *OsMYB46* [19], show similar functions, suggesting that the functions of these MYB TFs in SCW regulation are conserved.

Although this transcriptional regulation mode is relatively conservative in plants, the transcriptional regulatory networks implicated by other secondary cell wall-related TFs are distinct across different plant species [6]. For example, only 2 of the 29 direct target genes mediated by *AtMYB46* were regulated by the *P. trichocarpa* homolog (*PtrMYB021*) [6]. The species-specific regulation of these TFs may explain the drastic divergence in secondary cell wall composition and physiological functions between conifers, herbaceous plants, and woody dicots. Therefore, to elucidate the transcriptional network, controlling wood formation in conifers is of paramount importance for future applications in fundamental tree biology and biotechnology.

Masson pine is an economically important industrial timber tree that is widely distributed in China. Compared with other timber trees, the relative cellulose content, average elastic modulus, and hardness of Masson pine wood were larger [20], and it has always been considered an important wood resource for the fiber (for pulp, paper products, and boards) and sawn timber (for building houses and furniture) industries in China [21]. Therefore, understanding the genetic regulation of SCW formation in Masson pine could inform TF modification strategies to improve the sustainable production of wood fiber and lumber. However, according to predictions, Masson pine has a large genome size of 22 Gb [22], and it is difficult to obtain the sequence in a short time [23]. The recalcitrance of Masson pine to genetic transformation and the lack of mutant collection also hinder genetic and functional genomic approaches to TF characterization [21]. These barriers hamper efforts to decipher the regulatory roles of TFs in wood formation of Masson pine. In this study, to expand our understanding of SCW formation, we carried out a functional analysis of MYB genes. Based on this conserved regulatory pattern between angiosperms and gymnosperms, we identified *PmMYB4*. Our expression analysis demonstrated that *PmMYB4* was highly expressed in lignin-forming tissues. Overexpression of *PmMYB4* in *Nicotiana benthamiana* induced ectopic SCW deposition, as was observed in *Arabidopsis* with overexpression of *AtMYB46* and *AtMYB83*, and transient co-expression analysis showed that *PmMYB4* up-regulated the promoter activities of the *PmCCoAOMT* and *PmPAL*. These results strongly suggested that *PmMYB4* plays an important role in secondary wall formation.

2. Results

2.1. Isolation and Characterization of *PmMYB4*

A putative R2R3-MYB TF gene was obtained by BLAST searching in the Masson pine database (PRJNA655997) [24] using *PgMYB4* (accession no. ABQ51220.1) as a query sequence. The ORF was amplified from the leaf cDNA of 2-year-old Masson pine by RT-PCR. The obtained sequence, named *PmMYB4*, encoded a deduced polypeptide of 490 amino acid residues with a calculated molecular weight of 54.2 KD and an isoelectric point of 5.43.

The N-terminus of *PmMYB4* contained typical R2R3 imperfect repeats, which mediate binding to target DNA sequences and are highly conserved among R2R3-MYB proteins (Figure S1). The comparison of the *PmMYB4* amino acid sequence with those of other MYB proteins showed high identity with lignin-associated MYB proteins from *Pinus taeda* (*PtMYB4*, 61.02%) and *Picea glauca* (*PgMYB4*, 64.08%) (Figure 1 and Figure S1).

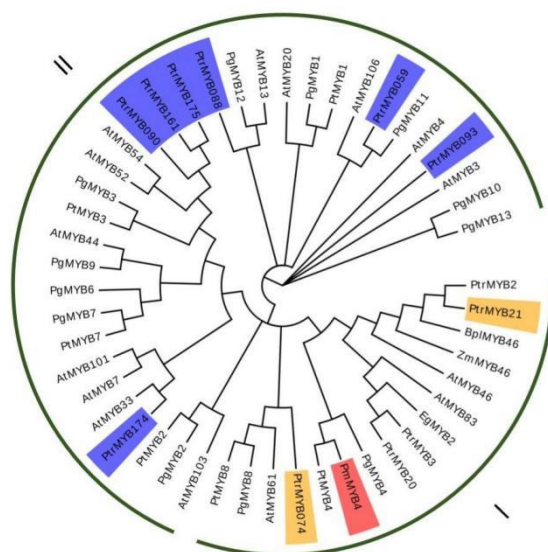


Figure 1. Phylogenetic analysis of *PmMYB4* with R2R3-MYB TFs involved in SCW formation in vascular plants. Phylogenetic tree analysis was performed with MEGAX. *PmMYB4* is highlighted with a red box; *PtrMYB21* and *PtrMYB074* (MYBs as secondary switches in the SCW pathway in *Populus trichocarpa*) are highlighted with orange boxes [6]; and *PtrMYB174*, *PtrMYB175*, *PtrMYB090*, *PtrMYB161*, *PtrMYB088*, *PtrMYB059*, and *PtrMYB093* (MYBs as tertiary switches in the SCW pathway in *Populus trichocarpa*) are highlighted with blue boxes [6]. Group I represents MYBs as secondary switches in the SCW, and group II represents other MYBs. The GenBank accession numbers of these R2R3-MYB TFs are listed in the Materials and Methods.

2.2. *PmMYB4* Is Primarily Expressed in Bark

We investigated the expression profiles of *PmMYB4* in various tissues of Masson pine by semiquantitative RT-PCR and quantitative real-time PCR. The results showed that *PmMYB4* was expressed in all tissues tested, but relatively high expression was found in bark, semi-lignified stems and new leaves (Figure 2). The highest level of *PmMYB4* expression was detected in bark, while the lowest was detected in roots and flowers. The *PmMYB4* transcript levels in bark were approximately 120-fold higher than those in flowers, while the transcript levels in semi-lignified stems were 47-fold higher (Figure 2). Although the expression of the *PmMYB4* gene was not xylem-specific, it was mainly expressed in lignin-forming tissues, such as semi-lignified stems and bark, suggesting that *PmMYB4* may play an important role in lignin biosynthesis during SCW formation.

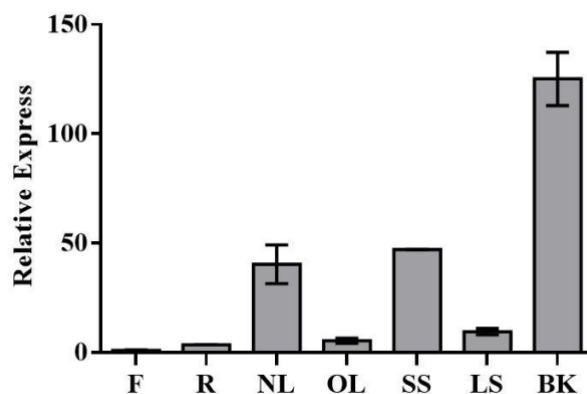


Figure 2. Tissue-specific expression patterns were characterized by real-time quantitative PCR, in which expression levels were averaged from three biological repeats and three technical repeats. Flowers (F), roots (R), new leaves (NL), old leaves (OL), semi-lignified stems (SS), lignified stems (LS), and bark (BK).

2.3. Transcriptional Activation of *PmMYB4* and the Binding Ability of *PmMYB4* with AC Elements

Yeast harboring pGBKT7-*PmMYB4* grew well on SD/-4 medium and turned blue on SD/-4 medium containing X- α -gal. The negative control transformed with pGBKT7 was unable to grow on SD/-4 medium (Figure 3A), indicating that *PmMYB4* has transcriptional activation activity. A yeast one-hybrid (Y1H) assay showed that cells transformed with pHISi-AC-I, pHISi-AC-II, pHISi-AC-III, or pHISi-SMRE4 and its corresponding mutated form pHISi-mAC grew well on SD/-Leu/-Trp medium but not on medium containing 40 mM 3-amino-1,2,4-triazole (3-AT) (Figure 3B). Bait Y1H cells (cells harboring AC elements or an mAC element) transformed with pGADT7-*PmMYB4* grew on SD/-Leu/-Trp/His medium. In contrast to cells expressing pHISi-mAC, cells expressing pHISi-AC-I, pHISi-AC-II, pHISi-AC-III, or pHISi-SMRE4 grew on medium supplemented with 40 mM 3-AT (Figure 3B), suggesting that *PmMYB4* could bind all four types of AC elements.

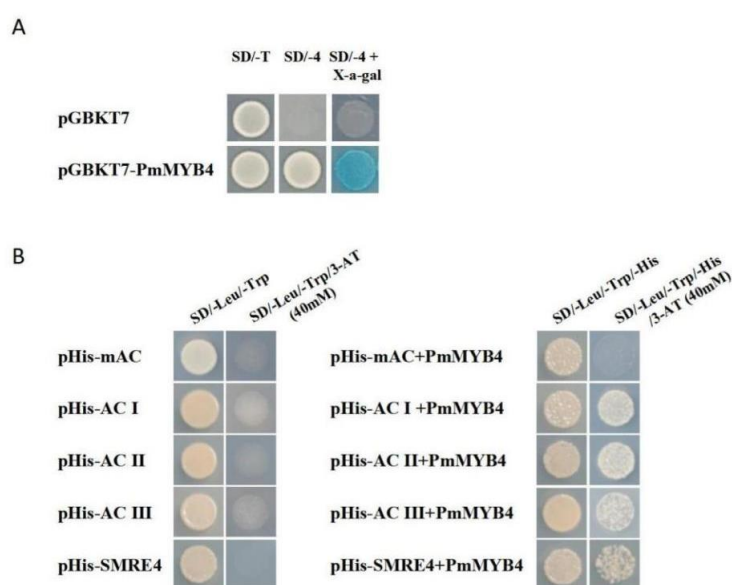


Figure 3. Transcriptional activation activity analyses of *PmMYB4* and DNA-binding assay of AC elements with *PmMYB4*. (A) Transcriptional activity analysis of *PmMYB4* via a yeast assay system, in which pGBKT7 was used as a negative control. (B) Y1H assay of *PmMYB4* with the four AC elements AC-I, AC-II, AC-III, and SMRE4, as well as their mutated forms, mAC.

2.4. Growth and Morphological Characteristics of *PmMYB4* Transgenic Tobacco

The results of RT-PCR and qRT-PCR indicated that the *PmMYB4* gene was integrated into the genomes of 6 independent transgenic plant lines and highly expressed in L1, L5, and L6 (Figure 4A,B). To investigate whether the overexpression of *PmMYB4* could impact plant growth, we monitored the individual growth of three transgenic plants (T1) from three lines and untransformed controls. Two months after planting in the soil, significant growth phenotype differences were observed between plants overexpressing *PmMYB4* and the wild type (WT). Height measurements of the 3 lines clearly indicated that L1, L5, and L6 plants were significantly shorter than WT plants (Figure 4C,D). Similarly, the transgenic lines had a significantly greater stem diameter (18.75%) than the WT (Figure 4E). In addition, the overexpression lines produced fewer leaves (33.03%) than the WT (Figure 4F). Generally, compared to the WT, lines overexpressing the *MYB4* gene showed altered growth characteristics.

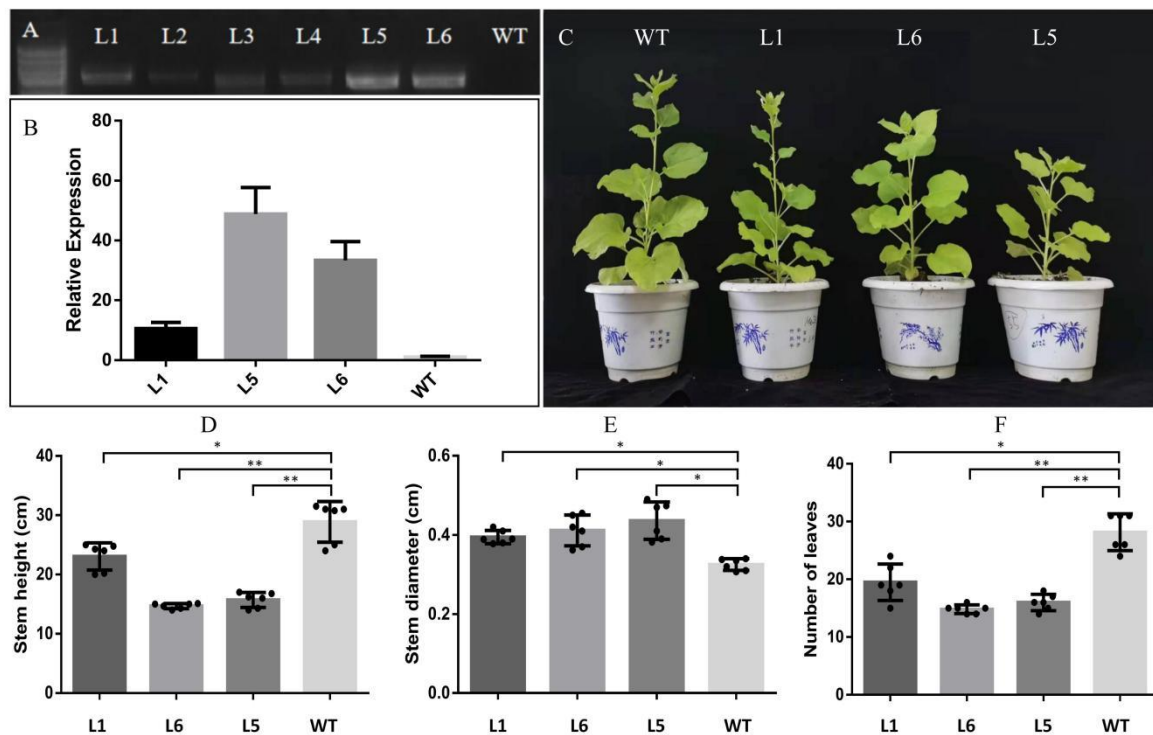


Figure 4. Phenotypic changes in *PmMYB4* transgenic lines. (A) Verification of *PmMYB4* tobacco transgenic lines by PCR amplification. Genomic DNA was extracted from the leaves of 1-month-old transgenic tobacco plants. The PCR products were assessed by electrophoresis on a 1.0% agarose gel. (B) Relative expression levels of *PmMYB4* in different transgenic lines characterized by real-time quantitative PCR, in which expression levels were averaged from three biological repeats and three technical repeats. (C) Phenotypic comparison of 2-month-old tobacco transgenic lines 1, 5, and 6 and the WT. Transgenic lines and WT plants were compared for three growth traits: (D) height, (E) stem diameter, and (F) number of leaves. The significance of differences between different lines was tested with the *t*-test. Asterisks represent significant differences between each OE line and WT (* $p < 0.05$, ** $p < 0.01$). The raw data is marked as a point on the histogram (D–F). WT represents wild-type tobacco, while the other lines labeled with line numbers are different *PmMYB4* tobacco transgenic lines. Each line contains six technical replicates.

2.5. Overexpression of *PmMYB4* Positively Regulates SCW in Transgenic Tobacco

The three independent lines (L1, L5, and L6) had similar phenotypes, and L5, which showed the highest expression (Figure 4B), was used for histochemical staining. In sections stained with phloroglucinol, which stains lignin, gray staining was more intense in the OE lines (Figure 5a,b). These results indicated that higher lignin deposition occurred in the OE lines than in the WT. We also found significantly increased lignin contents in the OE lines, as determined by chemical analysis (Table 1), which was consistent with the results of sections stained with phloroglucinol (Figure 5a,b). The chemical analysis also suggested that the cellulose content in the OE lines was higher than that in the WT. However, there were no differences in hemicellulose content among the WT and *PmMYB4*-overexpressing lines (Table 1). These results indicate that *PmMYB4* has a positive effect on lignin and cellulose contents but no obvious effect on the hemicellulose content.

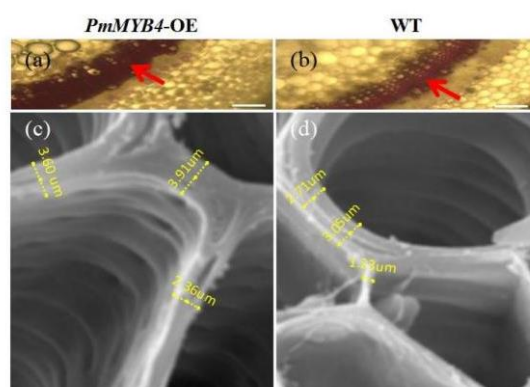


Figure 5. Sections stained with phloroglucinol-HCl and scanning electron micrographs of the 3rd internodes of control and transgenic-line plants. (b,d) Wild-type tobacco plants; (a,c) transgenic lines. The red arrow marks the site of lignin deposition (a,b). Short yellow lines in (c,d) indicate differences in cell wall thickness between the transgenic-line and wild-type plants. Bars = 20 μm (a,b).

Table 1. Secondary cell wall composition of transgenic and WT tobacco plants.

Samples	Lignin (%)	Cellulose (%)	Hemicellulose (%)
WT	21.56 \pm 0.16	42.17 \pm 0.92	24.56 \pm 1.0
L1	22.80 \pm 0.11 *	42.38 \pm 0.97	25.41 \pm 1.7
L5	25.09 \pm 0.32 *	44.56 \pm 0.36 *	24.16 \pm 2.8
L6	24.80 \pm 0.11 *	44.34 \pm 0.97 *	24.45 \pm 1.3

Measurements were conducted on transgenic tobacco plants overexpressing *PmMYB4* and WT plants. Expression levels were averaged from three biological repeats and six technical repeats. Values represent the mean and standard deviation. The significance of differences between different lines was tested with the *t*-test. Asterisks represent significant differences between each OE line and WT (* $p < 0.05$). All transgenic lines displayed significantly different values from the WT.

Increases in cell wall thickness result from increased deposition of xylose and cellulose [23]. To better understand the contribution of *PmMYB4* overexpression to SCW biosynthesis, microscopy analyses were conducted to measure the thicknesses of the stems of WT and transgenic plants. Notably, SEM images showed that the thickness of the entire cell wall, including the SCW, was greater in the overexpression lines than in the WT (Figure 5c,d). These results showed that overexpression of *PmMYB4* positively regulated SCW formation in transgenic tobacco.

2.6. Overexpression of *PmMYB4* Affects the Expression of SCW Biosynthesis Genes in Transgenic Tobacco

To better understand the molecular mechanisms of *PmMYB4*-mediated SCW formation, especially the accumulation of lignin and cellulose, we used qRT-PCR analysis to analyze the expression profiles of SCW biosynthetic genes. The results of qRT-PCR analysis showed that all detected lignin biosynthetic genes (*CCoAOMT1*, *CCoAOMT2*, *CCoAOMT3*, *PAL1*, *CAD-LIKE*, *HCT*, and *4CL*) presented significant expression increases in the *PmMYB4*-overexpressing transgenic lines. The expression of *CCoAOMT2*, *CCoAOMT3*, and *HCT* was upregulated five- to 20-fold in the transgenic lines (Figure 6). We also analyzed the expression profiles of *PAL4* and found no difference between the WT and *PmMYB4*-overexpressing transgenic lines (Figure 6). These results suggest that overexpression of *PmMYB4* in transgenic tobacco affected the expression of SCW-related genes.

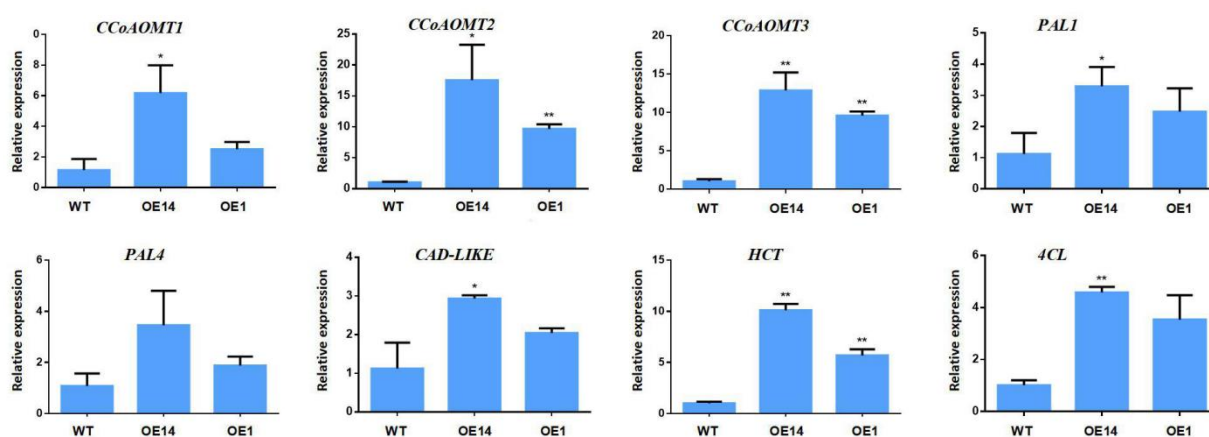


Figure 6. Expression profiles of SCW biosynthesis genes in WT and *PmMYB4*-overexpressing plants. *CCoAOMT1*, *CCoAOMT2*, *CCoAOMT3*, *PAL1*, *PAL4*, *CAD-LIKE*, *HCT*, and *4CL*: lignin biosynthetic genes. Gene expression profiles were evaluated by the $2^{-\Delta\Delta CT}$ method, and the gene expression levels in the WT were set as 1. Error bars represent \pm SD from three biological repeats and three technical repeats. The significance of differences between different lines was tested with the *t*-test. Asterisks represent significant differences between each OE line and WT (* $p < 0.05$, ** $p < 0.01$). The GenBank accession numbers of these SCW-related genes are listed in the Materials and Methods.

2.7. The *PmPAL* and *PmCCoAOMT* Promoters Are Activated by *PmMYB4*

To confirm that *PmMYB4* directly binds to the promoters of SCW biosynthesis genes, we conducted an analysis of cis-elements in the promoters of lignin biosynthetic genes (*PAL* and *CCoAOMT* genes). Then, a luciferase activity (LUC) assay was performed. A binary vector containing the CaMV 35S promoter and the CDS of *PmMYB4* was used as the effector, while vectors containing the two individual promoter fragments and LUC reporter genes were used as reporters (Figure 7B). Coexpression of effectors and reporters in the leaves of *Nicotiana benthamiana* significantly enhanced the relative LUC activity compared with that in mock-treated plants (Figure 7E). The results suggest that *PmMYB4* can bind to the promoters of lignin biosynthetic genes (*PAL* and *CCoAOMT*).

To further verify the above interactions identified in double-luciferase assays, the pBI121-NOGUS-*PmMYB4* construct was used as an effector, and two promoters were fused with the minimal 35S promoter to drive the GUS reporter gene (Figure 7B). GUS activity was detected in tobacco leaves following the co-transformation of lines harboring pBI121-NOGUS-*PmMYB4* with the two promoters. By analyzing the gray value of tobacco leaves, we found that the leaves co-transformed with 35S:*PmMYB4* and the promoter have darker GUS staining (Figure 7C,D). The results further showed that *PmMYB4* could activate the promoters of *PAL* and *CCoAOMT*.

In addition, the presence of an SNBE NAC binding site indicates that *PmMYB4* may be regulated by NAC as a secondary transcriptional switch in the SCW synthesis pathway of Masson pine (Figure 7F).

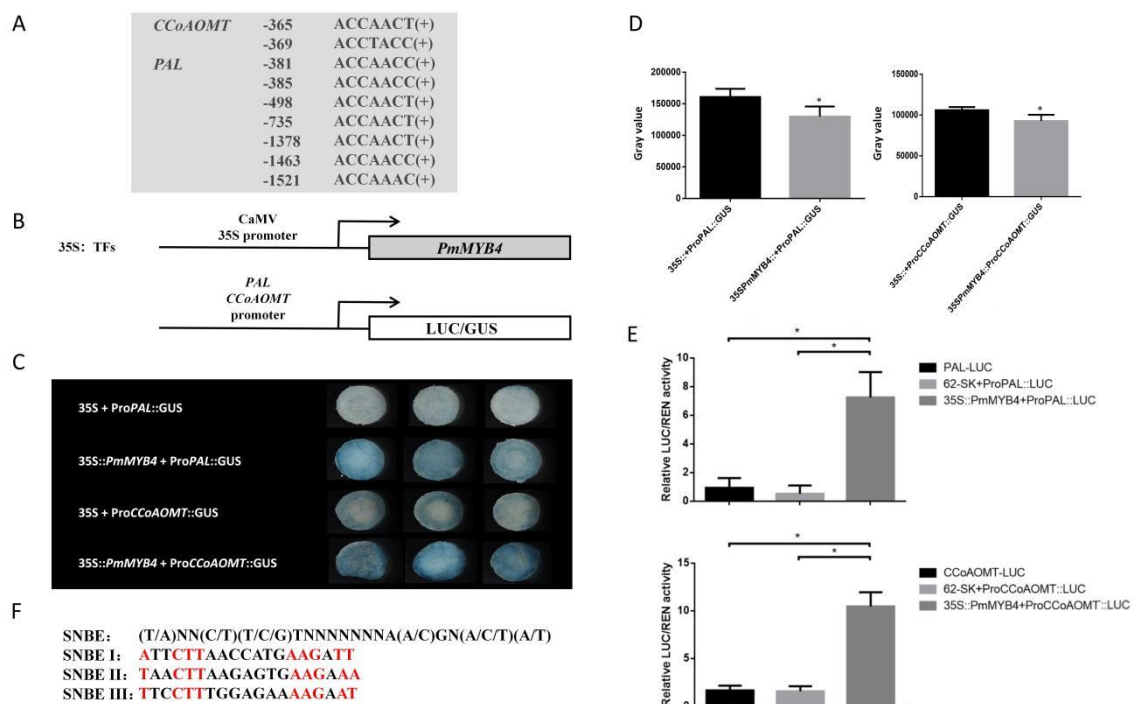


Figure 7. *PmMYB4* activates the promoters of *PmPAL* and *PmCCoAOMT*. **(A)** Identification of SMRE sequences in the promoters of representative direct *MYB4* targets based on the SMRE consensus sequence. The numbers shown to the left of each sequence represent the position of the first nucleotide relative to the start codon. The plus symbol on the right indicates the SMRE sequence from the forward strand of DNA. **(B)** Schematic diagram of the effector and reporter constructs used for coexpression in tobacco plants. **(C,D)** GUS staining, and **(E)** LUC activity. **(F)** Three SNBE motif sequences in the *MYB4* promoter. **(D)** The gray value of GUS was analyzed by IMAGEJ. The error bars indicate the standard deviation (SD) from three biological replicates. The significance of differences between different lines was tested with the *t*-test. Asterisks represent significant differences between experimental group and control group (* $p < 0.05$). The GenBank accession numbers of *PmPAL* and *PmCCoAOMT* are listed in the Materials and Methods.

3. Discussion

The identification of the molecular switches that regulate secondary cell wall biogenesis during wood formation is essential for basic studies and also for the biotechnological manipulation of wood quality and quantity in woody plant species [25]. While the TF-mediated transcriptional regulation of wood formation has been well studied in angiosperms [25–27], the understanding in conifers remains limited. Efforts to unravel the molecular regulation of coniferous secondary cell wall formation has implicated the R2R3-MYB family of TFs as transregulators of lignin biosynthesis and wood formation [28–32]. In this study, we elucidated a key TF, *PmMYB4*, associated with cell wall biogenesis in Masson pine and inferred an evolutionarily conserved regulatory mechanism of this TF on secondary cell wall formation. This study represents an important step towards understanding the coordinated transcriptional regulation that SCW formation in conifers.

Amino acid sequence alignment showed that the N-terminal region of *PmMYB4* contains R2 and R3 domains that are conserved with their homologous genes but differ in the C-terminal region (Figure S1). By subcellular localization and yeast one-hybrid assays, we determined that *PmMYB4* is a transcriptional activator that targets the nucleus. Tissue expression pattern analysis showed that *PmMYB4* was preferentially expressed in bark and semi-lignified stems. Interestingly, the expression level of *MYB4* in young tissues was higher than that in mature tissues, suggesting that *MYB4* may play an important role in plant growth and development.

One common strategy for functional characterization of a candidate gene is to down- or up-regulate its expression by genetic transformation. The long generation time and long life span of conifers have been major obstacles to perform reverse genetic approaches in these

woody plants [25]. Akiyoshi et al. (2019) avoided these difficulties by using heterologous expression of loblolly pine VNS genes in tobacco and *Arabidopsis* cells to infer TF functions regulating tracheid cell wall biosynthesis [33]. In this study, we produced transgenic tobaccos overexpressing the *PmMYB4* gene derived from *P. massoniana* under the control of a constitutive 35S promoter via *Agrobacterium*-mediated transformation [34]. The transgenic plants were significantly shorter than the WT plants, but the stems of the transgenic plants were thicker, similar to *AtMYB46* and *EgMYB2* [15,35]. In *Arabidopsis*, up-regulation of *AtMYB46* resulted in thickening of ectopic secondary wall observed in epidermis, cortex, and pith cells of stem cross-sections, and the severity of the ectopic secondary wall thickening phenotypes (e.g., dwarfing, leaf curling) was positively associated with the level of expression of the introduced *MYB46* gene [9]. Goicoechea found that half the tobaccos transformed with the *EgMYB2* construct (9/18) grew to only two-thirds of the size of the control plants. He believes that this phenomenon is related to the loss of top advantage [15]. Although the leaves showed signs of dysplasia, it was found that *PmMYB4* overexpressors did not exhibit the curly leaf phenotype, which is typical of the *MYB46* overexpressors (Figure 4C,F). Recently, it has been proposed that *PpMyb4* and its orthologs, *AtMYB46* and *EgMyb2*, could be nonspecific for regulating lignin biosynthesis because they are also involved in the regulation of cellulose and xylan biosynthesis [1]. To further verify whether *PmMYB4* has similar functions to *AtMYB46*, section staining, scanning electron microscopy and lignin, cellulose, and hemicellulose content analyses were performed on the overexpression lines. Overexpression of *PmMYB4* resulted in a thicker xylem and ectopic deposition of lignin (Figure 5a,b), which were consistent with the results of lignin content measurements (Table 1). Interestingly, the cellulose content in *PmMYB4*-overexpressing transgenic lines was also significantly increased, and the hemicellulose content did not change (Table 1). Previous studies have shown that *AtMYB46* and *EgMYB2* have a positive effect on hemicellulose content; however, Guo found that *BplMYB46* has a negative effect on hemicellulose content [16]. Whether this could be a subfunctionalization remains to be further studied. In addition, several genes involved in the secondary wall biosynthesis were up-regulated in transgenic tobaccos. Key genes for enzymes of monolignol biosynthesis, such as *CCoAOMT1*, *CCoAOMT2*, *CCoAOMT3*, *PAL1*, *PAL4*, *CAD*-like, or *HCT*, were up-regulated in the transgenic plants.

It is interesting to note that the SMRE consensus sequences include three variants that are identical to the AC elements (AC-I, ACCTACC; AC-II, ACCAACC; and AC-III, ACCTAAC) that were previously known to be involved in the activation of lignin and other phenylpropanoid biosynthetic genes [35–37]. Since R2R3 MYB DNA-binding domains are highly conserved in their sequences [13], it is not surprising to find that the homologous genes of *AtMYB46* bind to AC elements. Phylogenetic and expression analyses of *PmMYB4* have suggested a role as a potential candidate ortholog of *AtMYB46* genes regulating SCW formation (Figures 1, 6 and 7). The Y1H method showed that *PmMYB4* can bind to AC-boxes (AC-I, AC-II, AC-III, and SMRE4). The promoter region of the SCW gene was predicted from the loblolly pine genome, and seven AC-boxes and two AC-boxes were found in the promoter regions of *PAL* and *CCoAOMT*, respectively (Figure 7A). The promoter regions of *PmPAL* and *PmCCoAOMT* were cloned using Masson pine gDNA as the template with designed specific primers (Table S7). The results showed that the promoter regions of *PmPAL* and *PmCCoAOMT* contained AC-box motifs. To investigate whether *PmMYB4* can activate the promoters of *PmPAL* and *PmCCoAOMT*, MYB and promoter constructs were generated in the 35S effector vector and LUC/GUS reporter vector, respectively, and were then transformed into 5-week-old *N. benthamiana* leaves. The results were consistent with the Y1H assay, and the LUC/GUS activity assay confirmed that *PmMYB4* could activate the promoters of *PmPAL* and *PmCCoAOMT*. It is worth mentioning that the promoter of *PmMYB4* also contains 3 SNBE motifs (Figure 7F); however, whether *PmMYB4* is a target gene of PmSWNs remains to be further studied. The results obtained in this work suggested that a transcriptional cascade similar to the *AtMYB46* network defined in *Arabidopsis* [8,38] and poplar [39–41] is conserved in conifers.

The identification of *PmMYB4* as a main regulator of this network involved in wood formation in *P. massoniana* is of great interest for fundamental studies in conifers but also for potential applications in tree biotechnology. To increase our knowledge about the transcriptional regulatory network operating in conifers, and given the complexity of the network demonstrated in other species, intensive research is necessary to fully clarify to what extent the transcriptional network could be conserved between gymnosperms and angiosperms.

4. Materials and Methods

4.1. Plant Materials and Stress Treatments

Eight-year-old Masson pine trees were propagated at Nanjing Forestry University (NJFU) in Jiangsu Province, China. Seven tissues, including flowers, roots, new leaves, old leaves, semi-lignified stems, lignified stems, and bark, were directly frozen in liquid nitrogen and stored at $-80\text{ }^{\circ}\text{C}$ until RNA extraction. Total RNA was isolated from each sample using an RNAPrep Pure Plant Kit (Polysaccharides & Polyphenolics-rich) (Tiangen Biotech, Beijing, China) following the manufacturer's instructions.

Nicotiana benthamiana seedlings were planted in an artificial illumination incubator under appropriate conditions ($22\text{ }^{\circ}\text{C}$ with a 16-h light and 8-h dark photoperiod). Seeds were sterilized with 10% NaClO for 15 min and then sown in 1/2 MS medium. After 2 days of vernalization ($4\text{ }^{\circ}\text{C}$ dark), we placed the samples in an incubator for one week. At nine days after sowing (DAS), we transplanted the seedlings into a substrate (mixture of 60% turf soil, 30% pearlite, and 10% vermiculite).

4.2. Cloning of the Full-Length *PmMYB4* Coding Sequence (CDS) and Promoter

PmMYB4 was cloned from a cDNA library constructed from RNA isolated from needle tissue using the Prime Script 1st Strand cDNA Synthesis Kit (Takara, Dalian, China). A pair of primers was designed according to the full-length coding region of the *MYB4* gene sequence of *P. taeda* (GenBank: DQ399059.1). The PCR products were cloned into the pEASYT1 (Transgen, Beijing, China) vector, transformed into *E. coli* DH5 α , and then sequenced. All primers used in these assays are listed in Supplementary Table S1. The molecular weight and isoelectric point of the *PmMYB4* protein were determined using tools from the ExPASy website.

We extracted genomic DNA from 2-year-old Masson pine (DP320, Tiangen Biotech, Beijing, China) and isolated the 1781-bp promoter using three pairs of primers. The specific methods described in the Takara Genome Walking Kit instructions were followed. Based on the sequencing results, we designed a full-length specific primer Pro*PmMYB4*-F/R for the *PmMYB4* promoter to amplify the product of the full-length promoter. The online software PlantCARE (<http://bioinformatics.psb.ugent.be/webtools/plantcare/html/>) (accessed on 15 March 2021) was used to predict and analyze the cis-acting promoter elements. The primers are listed in Supplementary Table S1.

4.3. Sequence and Phylogenetic Analysis

The amino acid sequences of R2R3-MYB TFs were obtained from NCBI GenBank (<https://www.ncbi.nlm.nih.gov>) (accessed on 2 March 2021). Then, the sequences were used to construct a phylogenetic tree via the neighbor-joining (NJ) method using a Poisson model in MEGAX software (Park, PA, USA) [25] (<https://www.megasoftware.net/>) (accessed on 13 March 2021), and multiple sequence alignment was carried out with DNAMAN software [42]. The GenBank accession numbers of these R2R3-MYB TFs are listed in Section 4.12.

4.4. Transcriptional Activation Analysis of *PmMYB4*

The protein-coding region of *MYB4* was inserted into the pGBKT7 (Clontech, Shiga, Japan) vector (Table S2), and the construct was transformed into the yeast strain *Saccharomyces cerevisiae* AH109, together with pGADK7 by the LiAc/DNA/PEG method,

as described previously [43]. The transformed yeast cells were plated on SD/-T for the selection of positive clones and were then transferred to dropout SD4 medium lacking tryptophan (Trp), leucine (Leu), histidine (His), and adenine (Ade) for the transactivation assay. The empty pGBKT7 vector was used as the negative control.

To determine whether *PmMYB4* could bind AC elements, a yeast one-hybrid assay was performed using the Matchmaker Gold Yeast One-Hybrid Library Screening System (Clontech, USA) according to the manufacturer's protocol. Four forms of AC elements, i.e., AC-I (ACCTACC), AC-II (ACCAACC), AC-III (ACCTAAC), and SMRE4 (ACCAACT), are available thus far. Therefore, fragments containing three tandem repeat AC elements, AC-I, AC-II, AC-III, and SMRE4, and their mutated forms, mAC (ACCGAAT), were assembled into a pHISi vector. All primers used are listed in Table S5.

4.5. Semiquantitative RT-PCR and Quantitative Real-Time PCR

Total RNA was extracted from different tissues of Masson pine using the RNAPrep Pure Kit (DP441, Tiangen Biotech, Beijing, China). RNA concentrations and purity were measured with a NanoDrop 2000 instrument (Thermo Fisher Scientific, Waltham, MA, USA), and RNA integrity was estimated by 1.2% agarose gel electrophoresis [44]. First-strand cDNA was synthesized using the One-step gDNA Removal and cDNA Synthesis Kit (AT311, TransGen Biotech, Beijing, China). Primers were designed for quantitative real-time reverse transcription PCR (qRT-PCR) using Primer 5.0 (Table S4). SYBR Green reagents were used to detect the target sequences. Each PCR mixture (10 μ L) contained 1 μ L of diluted cDNA (20 \times dilution), 5 μ L of SYBR Green Real-time PCR Master Mix, 0.4 μ L of each primer (10 μ M), and 3.2 μ L of ddH₂O. The PCR program include six stages: (1) 95 $^{\circ}$ C for 60 s (predenaturation); (2) 95 $^{\circ}$ C for 15 s; (3) 60 $^{\circ}$ C for 15 s; and (4) 72 $^{\circ}$ C for 10 s, repeated 40 times (amplification); (5) 95 $^{\circ}$ C for 0.5 s; and (6) 60 $^{\circ}$ C for 1 min (melting). PCR product quality was estimated based on melting curve analysis. *TUA* (α -tubulin) was used as the internal control [44]. Three independent biological replicates and three technical replicates for each biological replicate were performed.

4.6. Agrobacterium-Mediated Transformation of Tobacco

The binary vector plasmid pBI121 harboring the desired *PmMYB4* gene (Table S4), in which *PmMYB4* was under the control of the CaMV 35S constitutive promoter, was introduced into *Agrobacterium tumefaciens* strain EHA105 by the freeze-thaw method [45]. Tobacco leaf discs were inoculated with an infective suspension (OD₆₀₀ = 0.6) of regenerated *A. tumefaciens* with gentle shaking at 200 rpm for 10 min. Then, the leaf discs were dried using sterile paper towels and co-cultivated on MS medium containing 0.4 mg/L N-6-benzyladenine (6-BA), 0.1 mg/L 1-naphthylacetic acid (NAA), 0.01 mg/L thidiazuron (TDZ), 6 g/L agar, 30 g/L sucrose, and 200 mM acetosyringone (AS) at pH 5.8 and incubated in the dark at 28 $^{\circ}$ C for 2 days. Subsequently, the leaf discs were transferred to MS medium supplemented with 0.4 mg/L 6-BA, 0.1 mg/L NAA, 6 g/L agar, 30 g/L sucrose, 400 mg/L cefotaxime, and 50 mg/L kanamycin at pH 5.8 under 16/8 h light/dark conditions at 25 \pm 1 $^{\circ}$ C in a phytotron to screen for putative transformant explants. Thereafter, the selected shoots were transferred first to half-strength MS rooting medium and then to soil and were propagated for complementary experiments. All transgenic and WT plants were acclimated and grown in a greenhouse at 18–23 $^{\circ}$ C under 60% humidity with 18 h of light and 6 h of dark daily at NJFU.

4.7. Plant Height and Biomass Measurements

The height from the basal stem to the tallest part of the plant and the stem diameter 5 cm above the soil were measured in 2-month-old tobacco plants from each transgenic and WT line. In addition, the number of leaves of each plant was recorded for comparison. Three lines are those that we chose, and each line contains six technical replicates.

4.8. Microscopy and Histochemistry

The stems (5th internode) of 2-month-old transgenic plants and WT plants were used for scanning electron microscopy (SEM) according to the protocol previously described by Yu et al. (2011) [46]. The image analysis software IMAGEJ (<https://imagej.nih.gov/ij/>) (accessed on 9 July 2021) was employed to quantify the morphological parameters of xylem cells (mm) and wall thickness.

Stems of 2-month soil-grown OE and WT *PmMYB4* tobacco plants were fixed in dyeing solution (25 mg phloroglucinol powder, 25 mL of 100% methanol, and 25 mL 37% glacial acetic acid), and sections were obtained via the freehand slicing method. The stem sections were stained with phloroglucinol-HCl and examined by light microscopy [9]. At least three technical replicates were performed in these experiments.

4.9. Measurement of Lignin, Cellulose, and Hemicellulose Components in Transgenic Tobacco

Sections were obtained via the freehand slicing method. The stem sections were stained with phloroglucinol-HCl and examined by light microscopy [47]. The acetyl bromide (AcBr) method was used to estimate the total lignin content [48]. Cellulose and hemicellulose contents were measured by the Van Soest method [49]. The percent contents of cellulose, lignin and hemicellulose determined in the three biological replicates, and six technical replicate experiments were then averaged.

4.10. Transient Expression and LUC/GUS Activity Assay

The full-length CDS of *PmMYB4* was amplified by PCR with gene-specific primers (Table S6) and then ligated into the plant binary vector pGreenII 62-SK driven by the CaMV 35S promoter. This construct was used as an effector in the LUC activity assay. Promoter fragments (*PAL* 1528 bp and *CCoAOMT* 646 bp) were independently cloned (Table S1) and ligated into the pGreen-0800-35 mini vector to produce various LUC reporters, and these constructs were used as effectors. All of these vectors were individually transformed into the *A. tumefaciens* strain GV3101. The effectors and reporters were infiltrated into the leaves of 2-week-old tobacco (*Nicotiana benthamiana*) plants by using the agroinfiltration method [50]. After 48 h of incubation, LUC activity was measured with a GloMax[®] 20/20 luminometer.

The *PAL* and *CCoAOMT* promoters were fused with the 35S CaMV minimal promoter to drive the expression of the GUS gene in the pBI121 vector using the primers listed in Table S7. The full CDS of *PmMYB4* was cloned into pBI121-NO-GUS under the control of the 35S promoter (35S:*PmMYB4*) as the effector. The reporters and effector were simultaneously infiltrated into the leaf epidermal cells of *N. benthamiana* as described above. After incubation at 28 °C for 2 days in the dark, blade samples with a diameter of 1 cm were collected with a hole punch and decolorized with 75% ethanol. Finally, GUS staining was performed under a stereomicroscope (SZX16, OLYMPUS, Tokyo, Japan) and a stereo-fluorescence microscope (M205FA, Leica, Wetzlar, Germany). The gray value of GUS was analyzed by IMAGEJ.

4.11. Statistical Analysis

All experimental data were obtained from at least three replicates, and statistical analysis was performed with Student's *t*-test. In all experiments, significant differences in the data were evaluated by one-way ANOVA. * $p < 0.05$, and ** $p < 0.01$.

4.12. GenBank Accession Numbers of Genes Used in This Study

The GenBank accession numbers of genes used in this study are as follows: *PgMYB1* (ABQ51217.1), *PgMYB2* (ABQ51218.1), *PgMYB3* (ABQ51219.1), *PgMYB4* (ABQ51220.1), *PgMYB6* (ABQ51222.1), *PgMYB7* (ABQ51223.1), *PgMYB8* (ABQ51224.1), *PgMYB9* (ABQ51225.1), *PgMYB10* (ABQ51226.1), *PgMYB11* (ABQ51227.1), *PgMYB12* (ABQ51228.1), *PgMYB13* (ABQ51229.1), *PtMYB1* (AAQ62541.1), *PtMYB2* (ABD60283.1), *PtMYB3* (ABD60282.1), *PtMYB4* (AAQ62540.1), *PtMYB7* (ABD60281.1), *PtMYB8* (ABD60280.1), *At-*

MYB3 (BAA21618.1), *AtMYB4* (BAA21619.1), *AtMYB7* (NP_179263.1), *AtMYB13* (NP_172108.1), *AtMYB20* (AEE34479.1), *AtMYB33* (Q8W1 W6.1), *AtMYB44* (Q9FDW1.1), *AtMYB46* (NP_196791.1), *AtMYB52* (NP_173237.1), *AtMYB54* (NP_177484.1), *AtMYB61* (NP_172425.2), *AtMYB83* (OAP02264.1), *AtMYB101* (NP_180805.1), *AtMYB103* (NP_176575.1), *AtMYB106* (NP_186763.2), *PtrMYB2* (AGT02397.1), *PtrMYB3* (KF148675.1), *PtrMYB20* (AGT02396.1), *PtrMYB21* (Potri.009G053900), *PtrMYB074* (Potri.015G082700), *PtrMYB059* (Potri.019G050900), *PtrMYB088* (Potri.018G095900), *PtrMYB090* (Potri.015G033600), *PtrMYB093* (Potri.004G138000), *PtrMYB161* (Potri.007G134500), *PtrMYB174* (Potri.017G037000), *PtrMYB175* (Potri.017G017600), *ZmMYB46* (AEO53061.1), *BplMYB46* (AKN79282.1) and *EgMYB2* (CAE09057.1), *CCoAOMT1* (NM_001325400.1), *CCoAOMT2* (U62734.1), *CCoAOMT3* (NM_001325467.1), *PAL1* (JK739025.1), *PAL4* (EU883670.1), *CAD-LIKE* (EH363427.1), *HCT* (AJ555865.1), *4CL* (XM_009800561.1), *Pm-CCoAOMT* (KF419292), and *PmPAL* (GQ142010).

Supplementary Materials: The following are available online at <https://www.mdpi.com/article/10.3390/f12121618/s1>. Table S1: Primer sequences used in cloning sequence, Table S2: Primer sequences used in the construction of pGBKT7-*PmMYB4*, Table S3: Primer sequences of genes analyzed by real-time RT-PCR, Table S4: Primer sequences used in the construction of *PmMYB4* overexpression lines, Table S5: Primer sequences used in the Y1H assay, Table S6: Primer sequences used in the LUC/GUS activity assay, Figure S1: Analysis of the *PmMYB4* promoter sequence.

Author Contributions: Conceptualization, S.Y.; software, S.Y. and Q.H.; investigation, S.Y. and J.L.; resources, P.C. and Y.Y.; writing—original draft preparation, S.Y. and M.Z.; writing—review and editing, S.Y. and K.J.; visualization, S.Y. and D.W. All authors have read and agreed to the published version of the manuscript.

Funding: The research was financially supported by the National Key R&D Program of China (2017YFD0600304) and the Priority Academic Program Development of Jiangsu Higher Education Institutions (PAPD).

Institutional Review Board Statement: Not applicable.

Informed Consent Statement: Not applicable.

Data Availability Statement: Not applicable.

Acknowledgments: The authors appreciate the support from Ziyuan Hao, Peihuang Zhu, Yu Chen, Yajin Ye, Ye Yang, Chi Zhang, Xuan Lou, and Yanqing Hou of The College of Forestry of Nanjing Forestry University. We would like to thank Major Biotechnology Corporation (Shanghai, China) for assistance with sequencing services.

Conflicts of Interest: The authors declare no conflict of interest.

References

- Plomion, C.; Leprovost, G.; Stokes, A. Wood formation in trees. *Plant Physiol.* **2001**, *127*, 1513–1523. [[CrossRef](#)]
- Blanch, H.W. Bioprocessing for biofuels. *Curr. Opin. Biotechnol.* **2012**, *23*, 390–395. [[CrossRef](#)] [[PubMed](#)]
- Cosgrove, D.J. Growth of the plant cell wall. *Nat. Rev. Mol. Cell Biol.* **2005**, *6*, 850–861. [[CrossRef](#)] [[PubMed](#)]
- Xu, C.Z. *PtoMYB170* positively regulates lignin deposition during wood formation in poplar and confers drought tolerance in transgenic *Arabidopsis*. *Tree Physiol.* **2017**, *37*, 1713–1726. [[CrossRef](#)] [[PubMed](#)]
- James, A.R.; William, R.A. Molecular evolution of the MYB family of transcription factors: Evidence for polyphyletic origin. *J. Mol. Evol.* **1998**, *46*, 74–83.
- Chen, H.; Wang, J.P.; Liu, H.Z.; Li, H.Y.; Lin, Y.C.; Shi, R.; Yang, C.M.; Gao, J.H.; Zhou, C.G.; Li, Q.Z.; et al. Hierarchical Transcription Factor and Chromatin Binding Network for Wood Formation in *Populus trichocarpa*. *Plant Cell* **2019**, *31*, 602–626. [[CrossRef](#)]
- Minoru, K.; Makiko, U.; Nobuyuki, N. Transcription switches for protoxylem and metaxylem vessel formation. *Genes Dev.* **2005**, *19*, 1855–1860.
- Zhong, R.Q.; Demura, T.; Ye, Z.H. *SND1*, a NAC domain transcription factor, is a key regulator of secondary wall synthesis in fibers of *Arabidopsis*. *Plant Cell* **2006**, *18*, 3158–3170. [[CrossRef](#)]
- Nobutaka, M.; Akira, I.; Hiroyuki, Y. NAC transcription factors, *NST1* and *NST3*, are key regulators of the formation of secondary walls in woody tissues of *Arabidopsis*. *Plant Cell* **2007**, *19*, 270–280.

10. De, R.B.; Mähönen, A.P.; Helariutta, Y. Plant vascular development: From early specification to differentiation. *Nat. Rev. Mol. Cell Biol.* **2016**, *17*, 30–40.
11. Ko, J.H.; Kim, W.C.; Kim, J.Y.; Ahn, S.J.; Han, K.H. MYB46-Mediated Transcriptional Regulation of Secondary Wall Biosynthesis. *Mol. Plant* **2012**, *5*, 961–963. [[CrossRef](#)]
12. McCarthy, R.L.; Zhong, R.; Ye, Z.H. MYB83 is a direct target of SND1 and acts redundantly with MYB46 in the regulation of secondary cell wall biosynthesis in *Arabidopsis*. *Plant Cell Physiol.* **2009**, *50*, 1950–1964. [[CrossRef](#)]
13. Zhong, R.; Ye, Z.H. Regulation of cell wall biosynthesis. *Curr. Opin. Plant Biol.* **2007**, *10*, 564–572. [[CrossRef](#)]
14. Zhong, R.; Ye, Z.H. MYB46 and MYB83 Bind to the SMRE Sites and Directly Activate a Suite of Transcription Factors and Secondary Wall Biosynthetic Genes. *Plant Cell Physiol.* **2012**, *53*, 368–380. [[CrossRef](#)]
15. Monica, G. EgMYB2, a new transcriptional activator from Eucalyptus xylem, regulates secondary cell wall formation and lignin biosynthesis. *Plant J.* **2005**, *43*, 553–567.
16. Guo, H.Y. Expression of the MYB transcription factor gene *BplMYB46* affects abiotic stress tolerance and secondary cell wall deposition in *Betula platyphylla*. *Plant Biotechnol. J.* **2017**, *15*, 107–121. [[CrossRef](#)]
17. Bomal, C.B.; Frank, C.S.; Mansfield, S.D. Involvement of *Pinus taeda* MYB1 and MYB8 in phenylpropanoid metabolism and secondary cell wall biogenesis: A comparative in planta analysis. *J. Exp. Bot.* **2008**, *59*, 3925–3939. [[CrossRef](#)] [[PubMed](#)]
18. Zhong, R.; McCarthy, R.L.; Haghghat, M. The poplar MYB master switches bind to the SMRE site and activate the secondary wall biosynthetic program during wood formation. *PLoS ONE* **2013**, *8*, e69219. [[CrossRef](#)]
19. Zhong, R.Q. Transcriptional activation of secondary wall biosynthesis by rice and maize NAC and MYB transcription factors. *Plant Cell Physiol.* **2011**, *52*, 1856–1871. [[CrossRef](#)]
20. Cai, S.; Guo, Y.; Li, Y. Intra-tree Variation in Viscoelastic Properties of Cell Walls of Masson Pine (*Pinus Massoniana* Lamb). *J. Renew. Mater.* **2022**, *10*, 119–133. [[CrossRef](#)]
21. Ni, Z.; Han, X.; Yang, Z. Integrative analysis of wood biomass and developing xylem transcriptome provide insights into mechanisms of lignin biosynthesis in wood formation of *Pinus massoniana*. *Int. J. Biol. Macromol.* **2020**, *163*, 1926–1937. [[CrossRef](#)] [[PubMed](#)]
22. Morse, A.M.; Peterson, D.G.; Nurul, I. Evolution of Genome Size and Complexity in *Pinus*. *PLoS ONE* **2009**, *4*, e4332. [[CrossRef](#)] [[PubMed](#)]
23. Yao, S.; Wu, F.; Hao, Q. Transcriptome-Wide Identification of WRKY Transcription Factors and Their Expression Profiles under Different Types of Biological and Abiotic Stress in *Pinus massoniana* Lamb. *Genes* **2020**, *11*, 1386. [[CrossRef](#)] [[PubMed](#)]
24. Wu, F.; Sun, X.; Zou, B.; Zhu, P.; Ji, K. Transcriptional Analysis of Masson Pine (*Pinus massoniana*) under High CO₂ Stress. *Genes* **2019**, *10*, 804. [[CrossRef](#)] [[PubMed](#)]
25. María, B.P.; María, T.L.; Blanca, C.B. *PpNAC1*, a main regulator of phenylalanine biosynthesis and utilization in maritime pine. *Plant Biotechnol. J.* **2017**, *16*, 1094–1104.
26. Yoshimi, N.; Masatoshi, Y.; Hitoshi, E. NAC-MYB-based transcriptional regulation of secondary cell wall biosynthesis in land plants. *Front. Plant Sci.* **2015**, *6*, 288.
27. Taylor-Teeples, M.; Lin, L.; de Lucas, M.; Turco, G.; Toal, T.W.; Gaudinier, A. An Arabidopsis gene regulatory network for secondary cell wall synthesis. *Nature* **2015**, *517*, 571–575. [[CrossRef](#)]
28. Liu, B.G.; Wang, J.P. Tracheid-associated transcription factors in loblolly pine. *Tree Physiol.* **2020**, *40*, 700–703. [[CrossRef](#)]
29. Patzlaff, A.; McInnis, S.; Courtenay, A.; Surman, C.; Newman, L.J.; Smith, C. Characterization of a pine MYB that regulates lignification. *Plant J.* **2003**, *36*, 743–754. [[CrossRef](#)]
30. Newkum, L.J.; Perazza, D.E.; Juda, L.; Campbell, M.M. Involvement of the R2R3-MYB, *AtMYB61*, in the ectopic lignification and darkphotomorphogenic components of the det3 mutant phenotype. *Plant J.* **2004**, *37*, 239–250. [[CrossRef](#)]
31. Bedon, F.; Grima-Pettenati, J.; MacKay, J. Conifer R2R3-MYB transcription factors: Sequence analysis and gene expression in wood forming tissues of white spruce (*Picea glauca*). *BMC Plant Biol.* **2007**, *7*, 17. [[CrossRef](#)] [[PubMed](#)]
32. Craven-Bartle, B.; Pascual, M.B.; Canovas, F.M.; Avila, C. A Myb transcription factor regulates genes of the phenylalanine pathway in maritime pine. *Plant J.* **2013**, *74*, 755–766. [[CrossRef](#)] [[PubMed](#)]
33. Akiyoshi, N.; Yoshimi, N.; Ryosuke, S.; Yusuke, K.; Misato, O.; Taku, D. Involvement of VNS NAC-domain transcription factors in tracheid formation in *Pinus taeda*. *Tree Physiol.* **2019**, *40*, 704–716. [[CrossRef](#)] [[PubMed](#)]
34. Schuetz, M.; Benske, A.; Smith, R.A.; Watanabe, Y.; Tobimatsu, Y.; Ralph, J.; Demura, T. Laccases direct lignification in the discrete secondary cell wall domains of protoxylem. *Plant Physiol.* **2014**, *166*, 798–807. [[CrossRef](#)]
35. Ko, J. Ectopic expression of MYB46 identifies transcriptional regulatory genes involved in secondary wall biosynthesis in *Arabidopsis*. *Plant J. Cell Mol. Biol.* **2010**, *60*, 649–665. [[CrossRef](#)]
36. Rogers, L.A.; Campbell, M.M. The genetic control of lignin deposition during plant growth and development. *New Phytol.* **2004**, *1*, 17–30. [[CrossRef](#)]
37. Zhong, R.; Ye, Z.H. Transcriptional regulation of lignin biosynthesis. *Plant Signal. Behav.* **2009**, *4*, 1028–1034. [[CrossRef](#)]
38. Stracke, R.; Werber, M.; Weisshaar, B. The R2R3-MYB gene family in *Arabidopsis thaliana*. *Curr. Opin. Plant Biol.* **2001**, *4*, 447–456. [[CrossRef](#)]
39. Lin, Y.C.; Li, W.; Sun, Y.H.; Kumari, S.; Wei, H.; Li, Q.; Tunlaya-Anukit, S. SND1 Transcription factor-directed quantitative functional hierarchical genetic regulatory network in wood formation in *Populus trichocarpa*. *Plant Cell* **2013**, *25*, 4324–4341. [[CrossRef](#)]

40. Wang, S.; Li, E.; Porth, I.; Chen, J.G.; Mansfield, S.D.; Douglas, C.J. Regulation of secondary cell wall biosynthesis by poplar R2R3 MYB transcription factor *PtrMYB152* in *Arabidopsis*. *Sci. Rep.* **2014**, *4*, 5054. [[CrossRef](#)]
41. Maleki, S.S.; Mohammadi, K.; Movahedi, A. Increase in cell wall thickening and biomass production by overexpression of *PmCesA2* in Poplar. *Front. Plant Sci.* **2020**, *11*, 110. [[CrossRef](#)] [[PubMed](#)]
42. Altschul, S.F.; Gish, W.; Miller, W.; Myers, E.W.; Lipman, D.J. Basic local alignment search tool. *J. Mol. Biol.* **1990**, *215*, 403–410. [[CrossRef](#)]
43. Gietz, R.D.; Schiestl, R.H. High-efficiency yeast transformation using the LiAc/SS carrier DNA/PEG method. *Nat. Protoc.* **2007**, *2*, 38–41. [[CrossRef](#)] [[PubMed](#)]
44. Zhu, P.H.; Ma, Y.Y.; Zhu, L.Z.; Chen, Y.; Ji, K.S. Selection of suitable reference genes in *Pinus massoniana* Lamb. under different abiotic stresses for qPCR normalization. *Forests* **2019**, *10*, 632. [[CrossRef](#)]
45. Holsters, M.; De Waele, D.; Depicker, A.; Messens, E.; Van Montagu, M.; Schell, J. Transfection and transformation of *Agrobacterium tumefaciens*. *Mol. Gen. Genet.* **1978**, *163*, 181–187. [[CrossRef](#)]
46. Yu, Y.; Zhao, Y.Q.; Zhao, B.; Ren, S.; Guo, Y.D. Influencing factors and structural characterization of hyperhydricity of in vitro regeneration in *Brassica oleracea* var. *italica*. *J. Plant Sci.* **2011**, *91*, 159–165. [[CrossRef](#)]
47. Li, C.; Wang, X.; Ran, L.; Tian, Q.; Fan, D.; Luo, K. *PtoMYB92* is a transcriptional activator of the lignin biosynthetic pathway during secondary cell wall formation in *Populus tomentosa*. *Plant Cell Physiol.* **2015**, *56*, 2436–2446. [[CrossRef](#)]
48. Iiyama, K.; Wallis, A.F. An improved acetyl bromide procedure for determining lignin in woods and wood pulps. *Wood Sci. Technol.* **1988**, *22*, 271–280. [[CrossRef](#)]
49. Van Soest, P.J.; Wine, R.H. Use of detergents in the analysis of fibrous feeds IV determination of plant cell-wall constituents. *J. Assoc. Anal. Chem.* **1967**, *50*, 50–55.
50. Yang, Y.; Li, R.; Qi, M. In vivo analysis of plant promoters and transcription factors by agroinfiltration of tobacco leaves. *Plant J.* **2000**, *22*, 543–551. [[CrossRef](#)]